16th World Conference on Earthquake, 16WCEE 2017
Santiago Chile, January 9th to 13th 2017
Paper N° 1508 (Abstract ID)
Registration Code: S-D1463170881

FUNDAMENTAL DYNAMICS OF 3-DIMENSIONAL SEISMIC ISOLATION

W. Eltahawy[(1)], K. Ryan[(2)], S. Cesmeci[(3)] and F. Gordaninejad[(4)]

[(1)] PhD Student, Department of Civil and Environmental Engineering, University of Nevada, Reno, USA, walaaeltahawy@nevada.unr.edu
[(2)] Associate Professor, Department of Civil and Environmental Engineering, University of Nevada, Reno, USA, klryan@unr,edu
[(3)] PhD Student, Department of Mechanical Engineering, University of Nevada, Reno, USA, cesmecis@gmail.com
[(4)] Professor, Department of Mechanical Engineering, University of Nevada, Reno, USA, faramarz@unr,edu

Abstract

Seismic isolation systems for buildings are generally selected to achieve higher seismic performance objectives, such as continued operation or immediate occupancy following a design earthquake event. However, recent large scale tests have suggested that these objectives may be compromised if the shaking includes large vertical acceleration components that are damaging to the nonstructural components and contents. Some research has been conducted to develop three dimensional isolation systems that can isolate the structure from both the horizontal and vertical components of ground motion. In several cases, systems have been proposed without much justification of the target design parameters. Rocking has been noted as a potential concern for structures with 3D isolation systems, and complex systems have been proposed to control the rocking.

In this study, the fundamental dynamic response of structures with 3D isolation systems is explored. Target horizontal and vertical spectra for a representative strong motion site were developed based on NEHRP recommendations, and horizontal and vertical ground motions were selected that best fit the target spectra when the same amplitude scale factor was applied to all three motion components. Using a simple model of a rigid block resting on linear isolation bearings, the following aspects are evaluated for a wide range of horizontal and vertical isolation periods: response modes and severity of rocking, horizontal and vertical displacement demands in the isolation bearings, and attenuation of both horizontal and vertical accelerations in the structure relative to the ground acceleration.

Preliminary results point to a number of useful observations. For example, rocking appears to be an issue only if the horizontal and vertical isolation periods are closely spaced. Helical spring isolation systems that have been applied to a few structures have this characteristic. However, if the horizontal isolation period is large relative to the vertical isolation period, troublesome rocking can be avoided. In addition, other researchers have proposed systems with vertical isolation periods on the order of 2 seconds, which require large displacement and damping capacity. However, preliminary results suggest that vertical isolation periods as low as 0.5 seconds will be effective in attenuating the vertical acceleration. Limiting the vertical isolation period will make design of a 3D isolation system more feasible with respect to vertical displacement capacity and avoiding rocking.

Keywords: Seismic isolation, Vertical, Structural dynamics

1. Introduction

Seismic isolation systems minimize the effect of an earthquake by providing a flexible interface that uncouples the structure from the ground. The flexible isolators (elastomeric or friction bearings) increase the structure period, leading to a reduction of the accelerations and forces in the structure that result from the earthquake. Increasing displacements are largely absorbed by the isolation devices. Traditional isolation systems control the effect of the ground motion horizontal component; but do not mitigate the vertical component of shaking.

Recently, a few studies elaborated that ground motion vertical component influences the structure behavior. Two separate research programs, one led by Japanese researchers and the other by coauthor Ryan, examined whether continued functionality could be realized in strongly shaken full-scale seismically-isolated buildings, and the response was compared to these buildings in a "fixed-base" condition [1-2]. Because the isolation systems mitigated the horizontal response of the building, the tests allowed, for the first time, the influence of strong vertical structural acceleration to be observed when the horizontal structural acceleration was constrained to relatively low levels. The nonstructural components and contents exhibited vulnerabilities that were directly correlated to the vertical excitation intensity and vertical vibration of the floor system.

To date, 3-dimensional (3D) isolation systems have been utilized mainly to satisfy the needs of nuclear facilities. Researchers from Japan have aggressively pursued 3D seismic isolation approaches for this purpose [3]. Two types of 3D seismic isolation systems have been proposed: 1) 3D base isolation of the entire building, and 2) vertical isolation of the main component combined with horizontal base isolation of the entire building. Three candidate devices have been developed for 3D isolation: a rolling seal type air spring, a hydraulic system, and a cable reinforcing air spring. The rolling seal type air spring is a steel/concrete cylinder lowered into an air cavity and attached with a rolling rubber seal, and is configured in series with a laminated rubber bearing for lateral isolation [4-5]. The cable reinforced air spring consists of an inner cylinder attached to the base and an outer cylinder attached to the structure separated by an air cavity bounded by a flexible rubber sheet [6-7]. Also used in series with laminated rubber bearings, the hydraulic system consists of load carrying hydraulic cylinders filled with nitrogen gas, to which fluctuating pressure can be transmitted by the attached accumulator units [8]. The proposed systems have vertical isolation periods on the order of 1-2 seconds, and generally utilize dampers (oil dampers or viscous wall dampers) and rocking suppression devices to control both vertical and rocking displacements. A related commercial solution for 3D isolation is available through Shimizu Corporation, and has been implemented in at least one 3-story apartment building [9-10]. These solutions are unlikely to be widely adopted due to their complexity and cost. Recently, researchers in China have proposed 3D isolation for long span reticulated or lattice roof structures by repackaging traditional isolation approaches into new devices [11-13].

While the above studies have focused on the development of vertical or 3D isolation devices, little work has been done to investigate the general dynamics of 3D isolation systems to select target design parameters. Zhou et al. [14] investigated the dynamics of vertical and 3D isolation systems for potential application to modern nuclear facilities. A 3D isolation system with a vertical period (T_V) of about 0.33 sec was found to be feasible for the studied nuclear power plant model, and could effectively reduce the vertical in-structure responses. A rocking effect was obvious when T_V increased to 1.0 sec, and vertical bearing displacements were at least as large as the horizontal displacements for $T_V = 2.3$ sec.

The objective of this study is to identify governing parameters of 3D isolation system that optimize the overall response of the structure, considering the tradeoffs between different displacements and accelerations. Parameters that define the 3D isolation system include horizontal and vertical isolation period (T_H and T_V) and damping ratios. Other relevant variables include site parameters, target spectra, and building height/width or aspect ratio. These parameters are varied widely to determine a suitable combination between both horizontal and vertical effects, and identify the parameters of an effective isolation system in both directions. The behavior of the structure is simulated as a 2D rigid block model implemented in MATLAB.

2. Site Parameters and Target Spectra

Target spectra were developed to represent the seismic hazard in the horizontal and vertical direction. A hypothetical site location and soil type were defined to obtain these target spectra. The hypothetical site was located in greater Los Angeles area on class (D) soil. This site has mapped Risk-Targeted Maximum Considered Earthquake (MCE_R), 5 percent damped spectral acceleration of S_S = 2.11g at short periods and S_1 = 0.74g at 1.0 sec period. MCE_R horizontal and vertical target spectra were calculated for this site according to ASCE 7-10 [15] and NEHRP 2009 [16]. The equations used to calculate the horizontal MCE_R spectrum (adjusted for site class effects) are illustrated in Fig. 1 [15], while the equations used to calculate the vertical MCE_R spectrum [6] are presented in Fig. 2. In these equations, $S_{MS} = F_a S_S$ and $S_{M1} = F_v S_1$ where F_a and F_v are site coefficients for short periods and 1.0 sec periods, respectively. For site class (D) and $S_S \geq 1.25$ g, $F_a = 1.0$ while $F_v = 1.5$ as $S_1 \geq 0.5$ g. According to Section 23 of [16], C_V is a vertical coefficient that depends on S_S and site class. From Figs. 1 and 2, the peak vertical to horizontal spectral acceleration (V/H) ratio is observed to be 0.8 C_V. For site class (D), C_V varies from 0.7 to 1.5 for 0.2 g $\leq S_S \leq$ 2.0 g; consequently the V/H ratio ranges from 0.56 to 1.2. C_V = 1.5 and V/H ratio = 1.2 whenever $S_S \geq$ 2.0 g. For this study, V/H ratio was taken to be 1.2, which represents near-fault ground motions with relatively large vertical components of shaking. The developed horizontal and vertical MCE_R spectra with 5% damping and V/H ratio equal to 1.2 are presented in Fig. 3. At longer periods, the vertical spectrum is controlled by the requirement V/H is not less than 0.5 [16], resulting in a small platform in the calculated vertical spectra between T_V = 0.49 and 0.5 sec (Fig. 3).

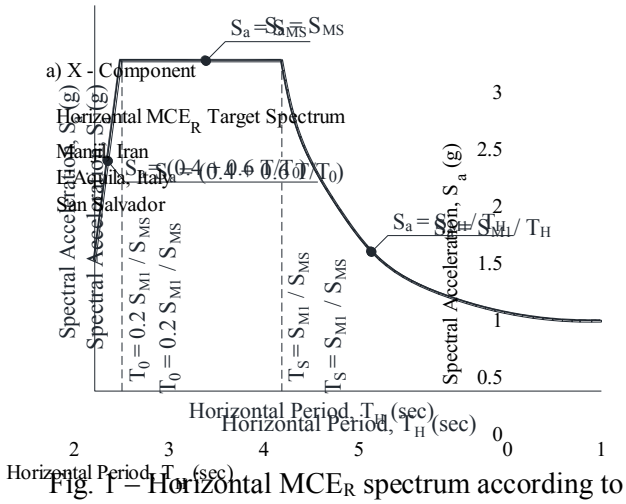

Fig. 1 – Horizontal MCE_R spectrum according to ASCE 7-10

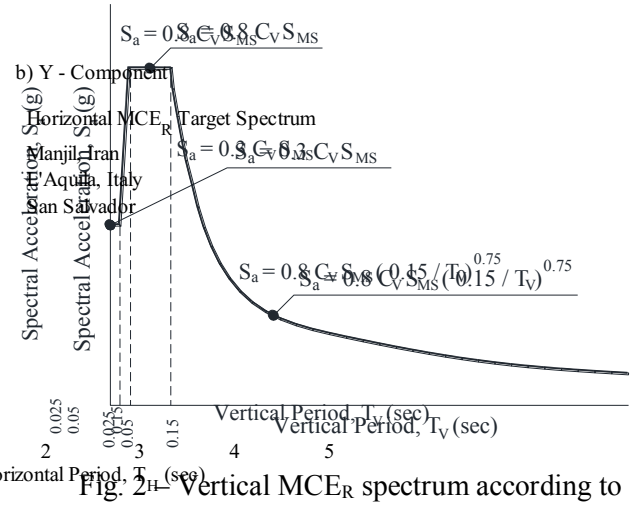

Fig. 2 – Vertical MCE_R spectrum according to NEHRP 2009

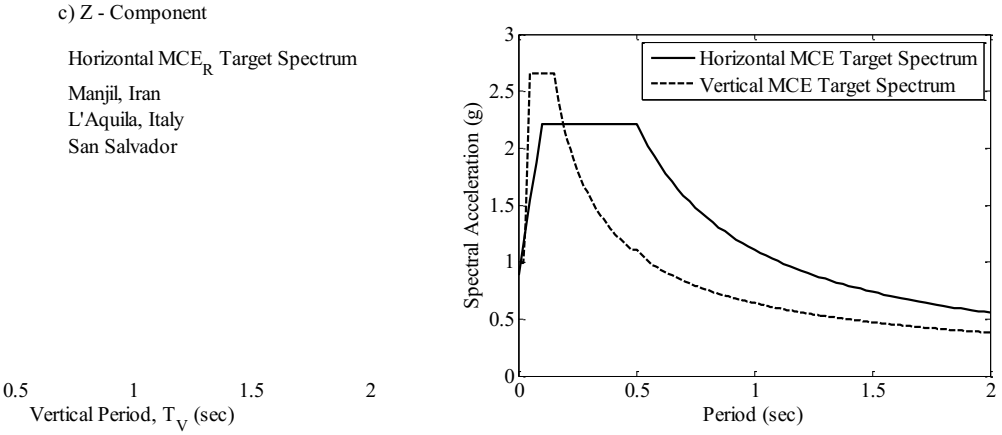

Fig. 3 – Horizontal and vertical MCE_R spectra with 5% damping

3. Ground Motion Selection and Scaling

A set of three motions with relatively large vertical components were hand selected to represent the target spectra, so that the effect of intense vertical shaking on the structure behavior can be studied. These motions

were amplitude-scaled to minimize the sum of the squared error between the scaled motion and the target spectrum over a wide period range. For reference, ASCE 7-10 requires that motions be scaled for periods ranging from 0.2 to 1.5 times the fundamental period of the structure for the direction of response being analyzed [15]. A broad period range was considered in both horizontal and vertical directions to accommodate the parameter variation considered in the study. The motions were scaled over a period range from 1.5 sec to 4.0 sec for the horizontal direction, and from 0 to 2.0 sec in the vertical direction.

This study utilizes a 2D model that will eventually extended to 3D; as such, all three components of ground shaking are considered. All three components were scaled by a single scale factor to preserve the relative component amplitudes of the original recorded motion. Table 1 summarizes the selected ground motions and the calculated scale factor. Scaled components of the selected three ground motion are compared to MCE_R spectra as presented in Fig. 4. The X and Y – components are compared to the horizontal MCE_R spectrum over the applicable period range, while the Z – component is compared to the vertical MCE_R spectrum. The scaled motions matched the target spectra well in both Y and Z directions; however, the Manjil, Iran record was below the target spectrum in the X – direction. Identifying motions that matched the target spectra well in three directions using a single scale factor was found to be difficult.

Table 1 – Selected ground motions

Earthquake	Year	Station	Scale Factor
San Salvador	1986	Geotechnical Investigation Center	2.6653
Manjil, Iran	1990	Abbar	1.8089
L'Aquila, Italy	2009	L'Aquila - Parking	2.8765

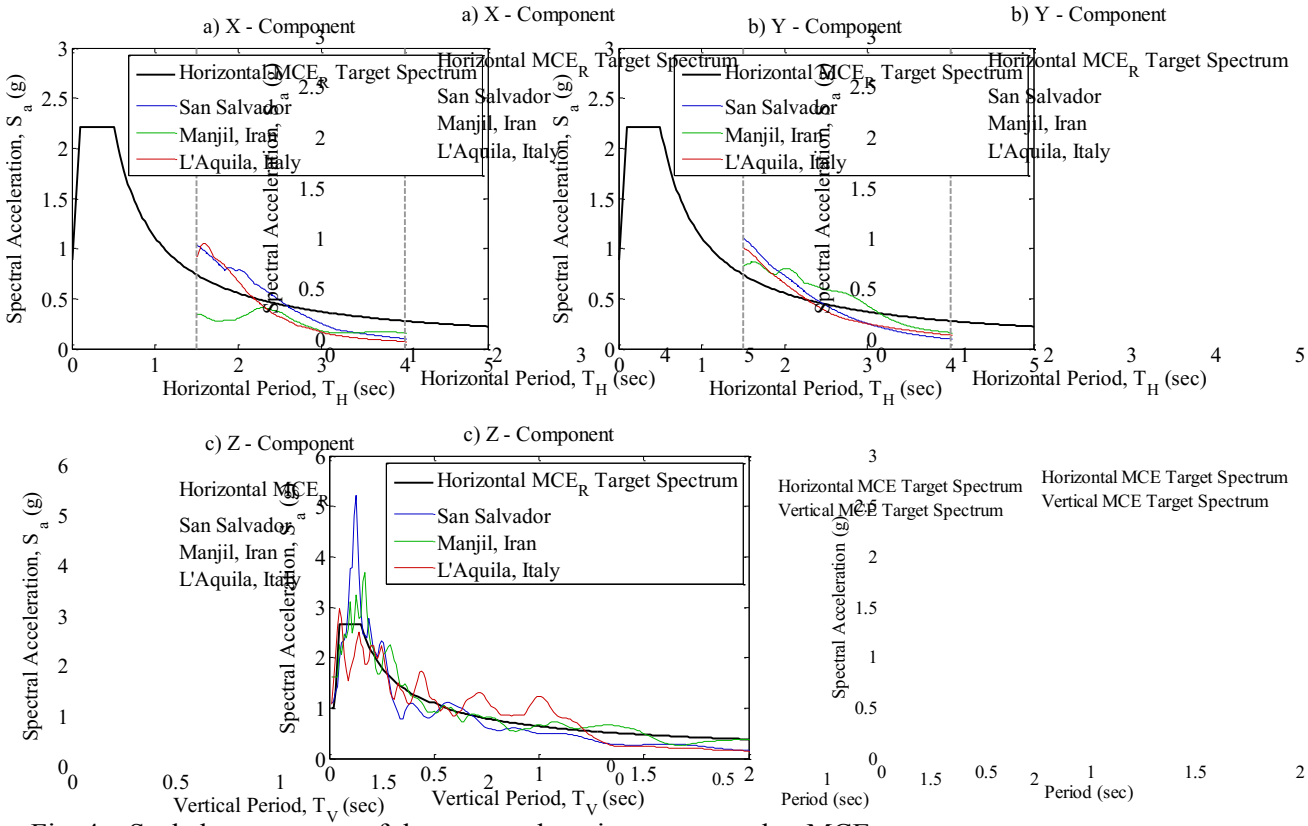

Fig. 4 – Scaled components of three ground motions compared to MCE_R target spectra a) X - Component, b) Y - Component and c) Z – Component

4. Numerical Modeling of the Isolated Rigid Block

4.1. Rigid block model

To obtain a basic understanding for fundamental dynamics of 3D isolation, a parameter variation study was performed on a simplified model of a building using MATLAB. The model is a 2D rigid block with an aspect ratio height:width = 2:1. This block is supported on isolation bearings at each base corner, represented by linear springs with total horizontal stiffness (K_H) and vertical stiffness (K_V), as shown in Fig. 5. The block dimensions are h = 20 m (height) and b = 10 m (width). The block has lumped mass (m) in the center with mass moment of inertia (I_θ). The model degrees of freedom (DOFs) are horizontal displacement (U_X), vertical displacement (U_Z), and rotation (θ) of the block (Fig. 5). The equations of motion for the system subjected to horizontal and vertical ground accelerations $\ddot{U}_{gx}(t)$ and $\ddot{U}_{gz}(t)$ is:

$$\begin{bmatrix} m & 0 & 0 \\ 0 & m & 0 \\ 0 & 0 & I_\theta \end{bmatrix} \begin{Bmatrix} \ddot{U}_x(t) \\ \ddot{U}_z(t) \\ \ddot{\theta}(t) \end{Bmatrix} + [C] \begin{Bmatrix} \dot{U}_x(t) \\ \dot{U}_z(t) \\ \dot{\theta}(t) \end{Bmatrix} + \begin{bmatrix} K_H & 0 & K_H * h/2 \\ 0 & K_V & 0 \\ K_H * h/2 & 0 & K_H * h^2/4 + K_V * b^2/4 \end{bmatrix} \begin{Bmatrix} U_x(t) \\ U_z(t) \\ \theta(t) \end{Bmatrix} = - \begin{bmatrix} m & 0 & 0 \\ 0 & m & 0 \\ 0 & 0 & I_\theta \end{bmatrix} \begin{Bmatrix} \ddot{U}_{gx}(t) \\ 0 \\ \ddot{U}_{gz}(t) \end{Bmatrix} \quad (1)$$

The damping matrix C is defined based on Rayleigh damping calibrated for target damping ratios in the first (horizontal) and second or third (vertical) mode. According to the stiffness matrix, horizontal translation and rocking are coupled, while the vertical translation is independent of rocking. The implemented equations of motion were solved in MATLAB numerically using Newmark's linear acceleration method (gamma (γ) = 1/2 and beta (β) = 1/6) with a time increment equal to the motion time step to minimize the error.

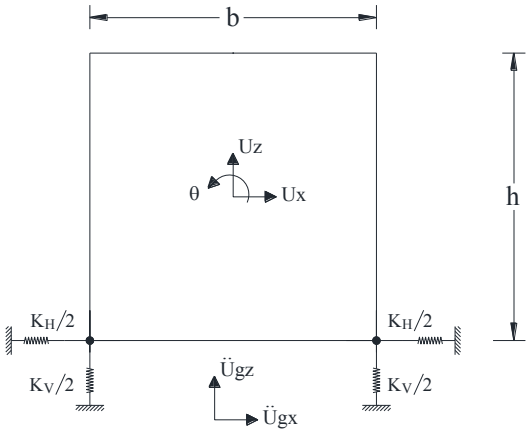

Fig. 5 – Rigid block used in MATLAB analysis

4.2. Modal analysis of rigid block

The behavior of the rigid block is investigated using X and Z components of scaled ground motions using two types of analyses. First, modal and time history analysis results are presented for the isolated rigid block subjected to the L'Aquila, Italy ground excitation only. The considered horizontal period (T_H) of the system is 3.0 sec, while the vertical period (T_V) is varied. The values of T_V are 0.1, 0.5, 1.0 and 2.0 sec while, and damping ratios are 20% in the horizontal and vertical modes (defined below). The modal analysis illustrates the contribution of the modes in the horizontal, vertical and rocking deformations. Table 2 summaries the relative displacements of each degree of freedom in each mode for various T_V. Fig. 6-9 present the response histories of the modal coordinates q in each mode and the displacements of each DOF for T_V = 0.1, 0.5, 1.0 and 2.0 sec, respectively. The modal coordinate q represents the contribution factor of each mode to the total deformation, but is sensitive to how the mode shapes are scaled.

The modes shall be referred to as horizontal (largest U_X), rocking (largest θ) and vertical (largest U_Z). Table 2 shows that the horizontal mode is always the first mode. The second mode is generally the rocking mode and the third mode is the vertical mode, except for T_V = 2.0 sec, where the rocking and vertical modes switch due to the increased flexibility of the vertical mode. Table 2 also shows that the rotation in the horizontal mode (relative to horizontal translation) increases with the increase of T_V, while the horizontal translation in the rocking mode (relative to rotation) increases with the increase of T_V. In other words, the coupling between horizontal translation and the block rotation increases with increase of T_V.

The response history results (Figs. 6-9) show that the coordinate $q_1(t)$ for the first (horizontal) mode does not vary much as the vertical period T_V is increased. As a result, the horizontal displacement U_X is not affected much by the vertical period. The amplitude of the coordinate $q_2(t)$ for the rocking mode (q_3 when T_V = 2 sec) increases substantially with each increase in vertical period, leading to a corresponding increase in rotation θ. For T_V = 2 sec (Fig. 9), the interaction between the horizontal and rocking modes is more apparent as U_X does not so closely resemble q_1 and θ does not so closely resemble the rocking mode q_3. For each case, the vertical displacement U_Z takes the exact shape of the vertical mode coordinate $q_3(t)$ (q_2 when T_V = 2 sec), and increases in amplitude while decreasing in frequency as T_V increases.

Table 2 – First three mode shapes

Case	Mode	Period (sec)	U_X	U_Z	θ
T_H = 3.0 sec, T_V = 0.1 sec	1st Mode	3.0067	1.0000	0	0
	2nd Mode	0.1288	0.0029	0	0.0043
	3rd Mode	0.10	0	-1.0000	0
T_H = 3.0 sec, T_V = 0.5 sec	1st Mode	3.1691	0.9978	0	-0.0003
	2nd Mode	0.6111	0.0669	0	0.0043
	3rd Mode	0.50	0	-1.0000	0
T_H = 3.0 sec, T_V = 1.0 sec	1st Mode	3.6825	0.9772	0	-0.0009
	2nd Mode	1.0517	0.2121	0	0.0042
	3rd Mode	1.0	0	-1.0000	0
T_H = 3.0 sec, T_V = 2.0 sec	1st Mode	5.4445	0.9121	0	-0.0018
	2nd Mode	2.0	0	-1.0000	0
	3rd Mode	1.4227	0.4100	0	0.0039

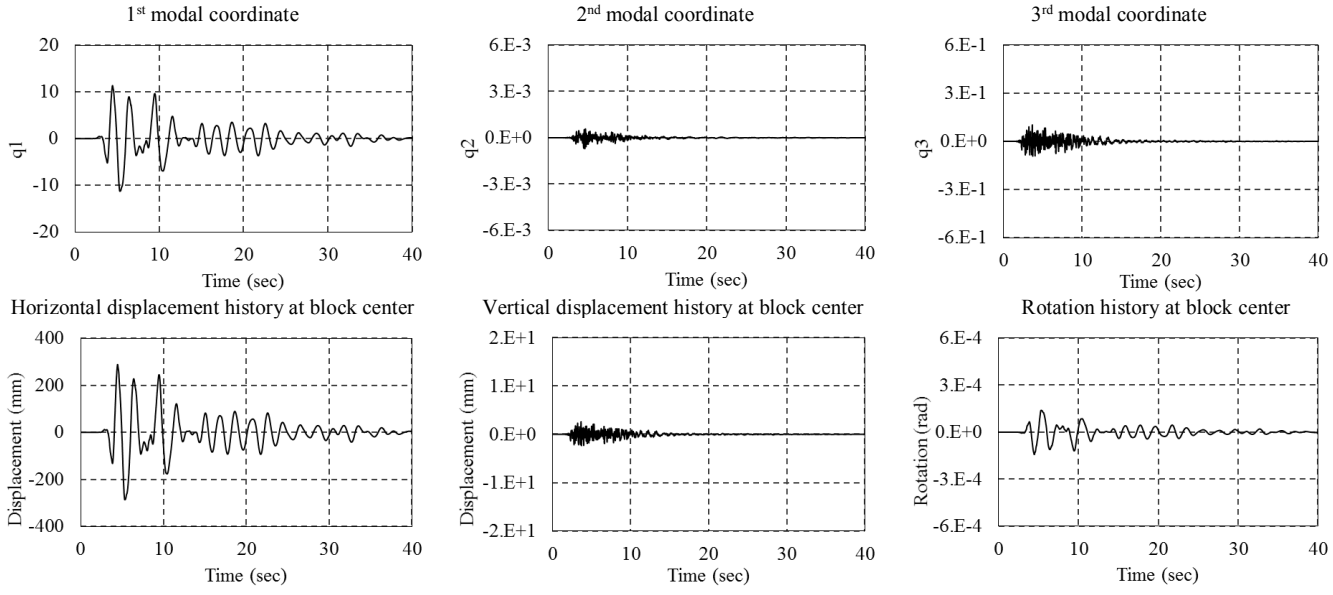

Fig. 6 – Modal and response history analysis results for vertical isolation period 0.1 sec

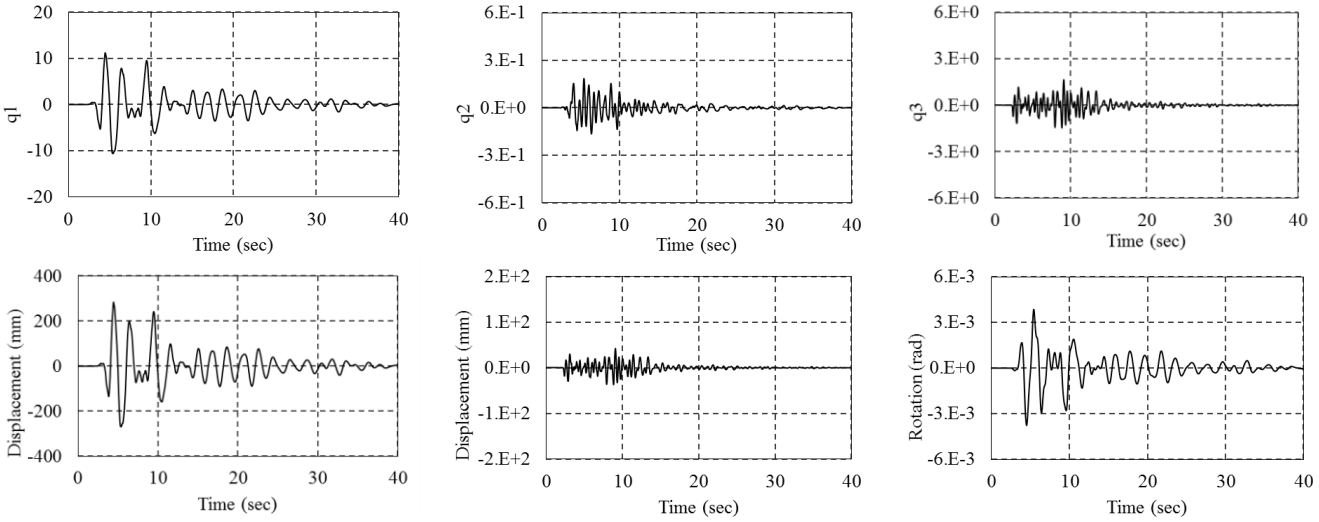

Fig. 7 – Modal and response history analysis results for vertical isolation period 0.5 sec

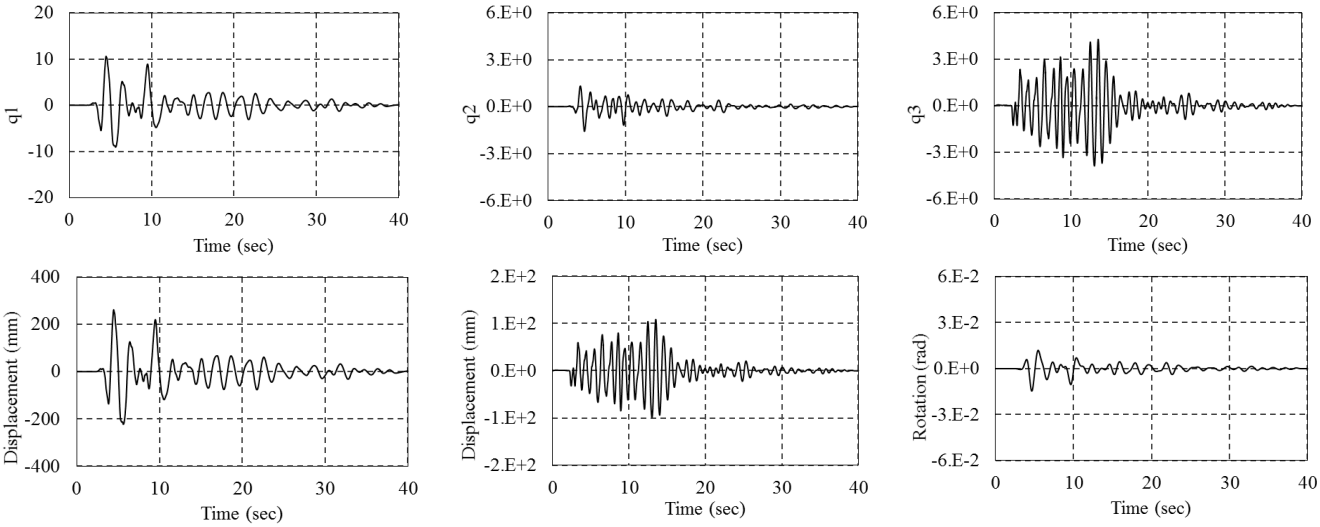

Fig. 8 – Modal and response history analysis results for vertical isolation period 1.0 sec

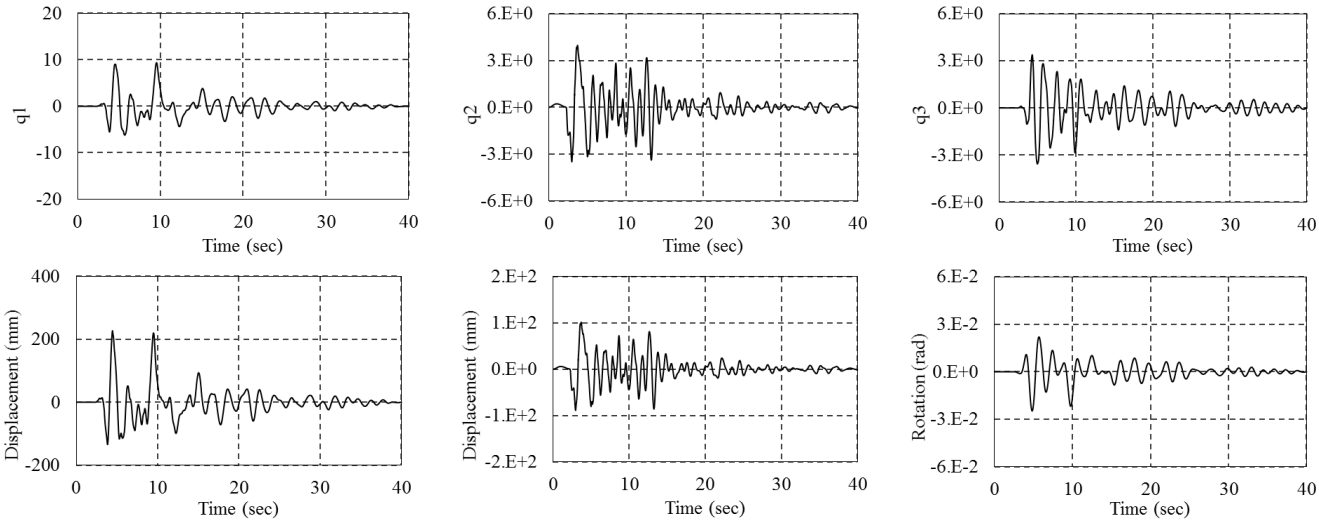

Fig. 9 – Modal and response history analysis results for vertical isolation period 2.0 sec

4.3. Seismic response of rigid block under parameter variation

Next, peak responses are presented for the three scaled ground motions as a function horizontal period T_H varying from 0 to 5 sec. $T_H < 1$ sec represents the response of a comparable fixed base structure. As before, discrete values of T_V = 0.1, 0.5, 1.0 and 2.0 sec are considered, and damping ratios of 20% are applied in the horizontal and vertical modes. The resulting peak horizontal displacement at the bearing, peak drift ratio (in percent), and peak vertical displacement from the static position at the left bearing are shown in Fig. 10, Fig. 11 and Fig. 12, respectively. Drift was computed as the ratio of relative horizontal displacement to the block height ($(U_{X\,Top} - U_{X\,Bottom})/h$), which the authors have found to be representative of actual drift for comparing simulation results between the rigid block model and a flexible structure.

The bearing horizontal displacement increases with the increase of T_H; however, it decreases with implementing higher values of T_V, as illustrated in Fig. 10. For example, at T_H = 3.0 sec, the bearing horizontal displacement due to San Salvador motion is 500, 450, 375 and 275 mm for T_V = 0.1, 0.5, 1.0 and 2.0 sec, respectively. Note that the bearing horizontal displacement is influenced by DOFs U_X and θ (shown in Figs. 6-9), and thus the decrease with increasing T_V is due to the increased influence of rocking. The drift ratio (Fig. 11) decreases with the increase of T_H, but is also coupled with T_V. Large drifts result even at low T_H when vertical flexibility is introduced (T_V = 0.5, 1 or 2 sec). In each case, the drift ratio is maximized approximately when $T_H = T_V$. However, the drift ratio always decreases as T_H increases beyond T_V. This suggests that for effective design, T_H and T_V should not be closely coupled, and T_H should be selected to be much longer than T_V. ASCE 07-10 states that the maximum story drift of the structure above the isolation system shall not exceed 1.5% [15]. Thus, T_V = 0.5 sec produces aceptable results for almost all T_H, T_V = 1.0 sec produces aceptable drifts for $T_H > 3$ to 4 sec, and T_V = 2 sec produces drift higher than ASCE limit for all values of T_H. Vertical displacement at the bearings is closely correlated to the drift as shown in Fig. 12. Bearings vertical displacement increases with the increase of T_V, however, it is almost linear with T_H except for T_V = 0.5 and 1.0 sec, vertical displacement at the bearings decreases as T_H increases. The choice of suitable T_V will also be influenced by the ability of the isolation system to accommodate such displacement.

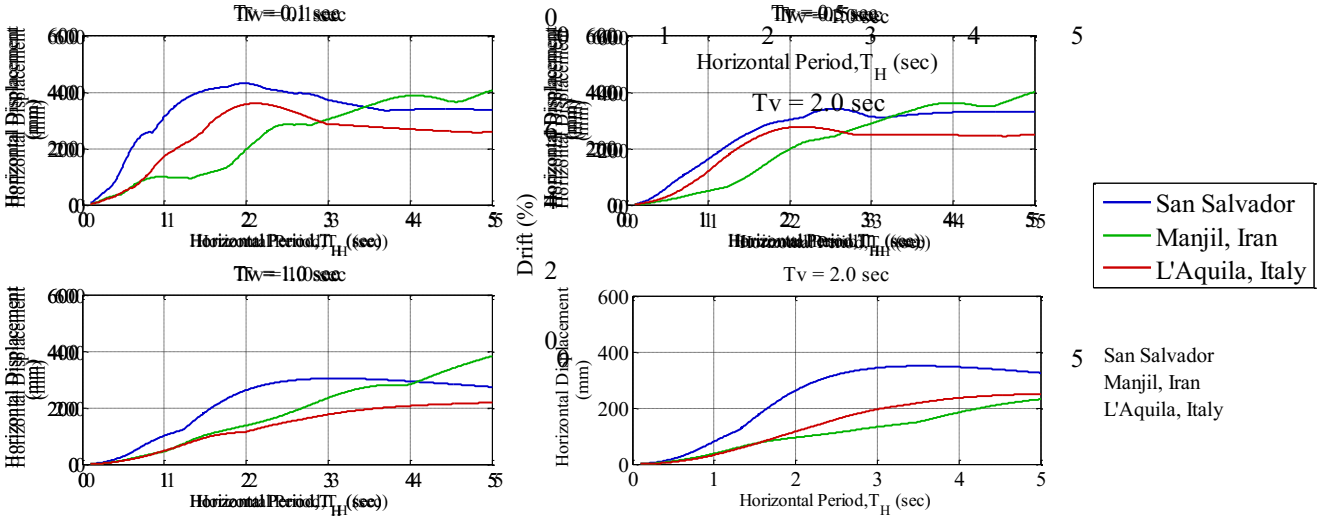

Fig. 10 – Horizontal displacement at the bearings

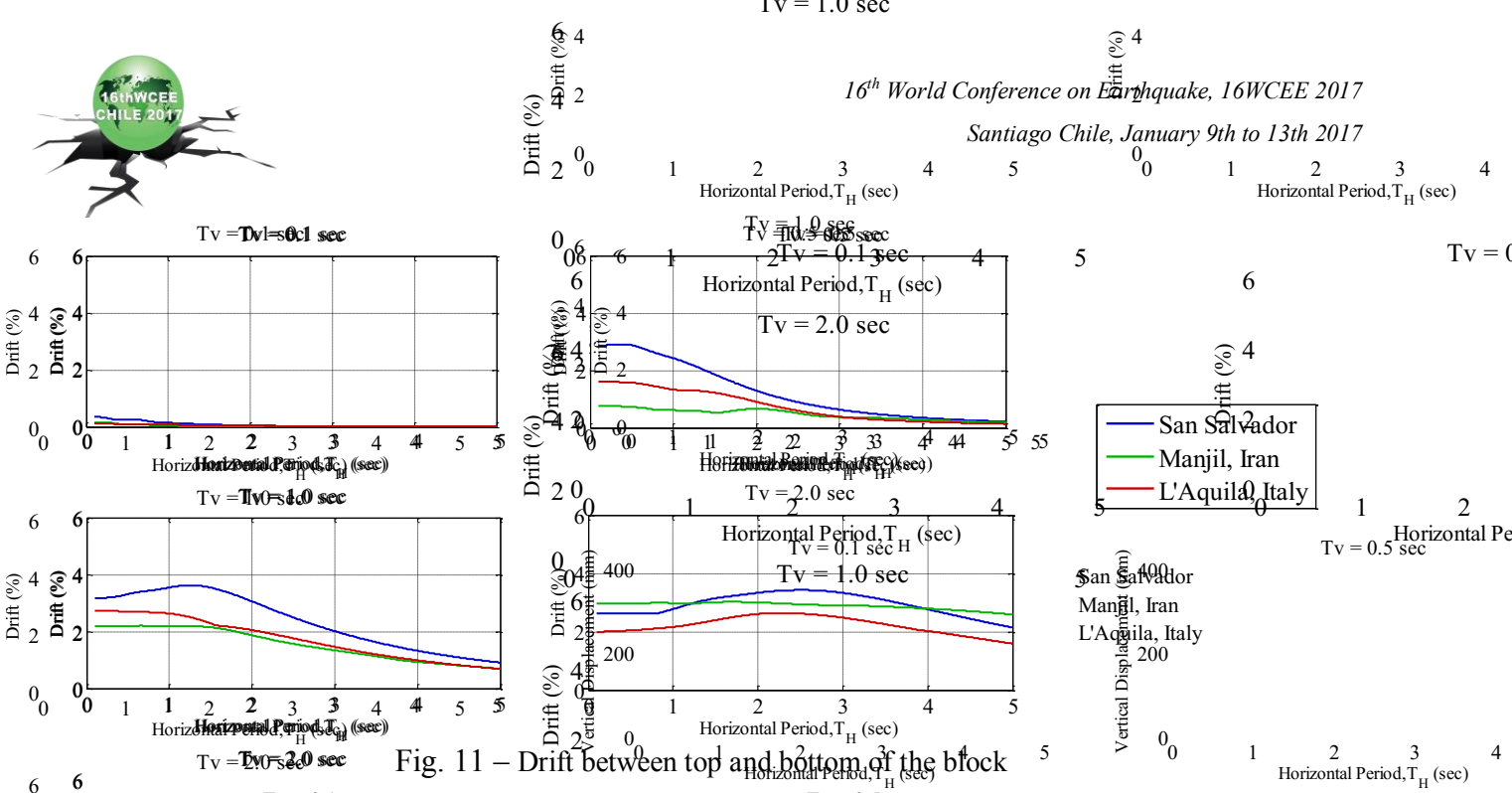

Fig. 11 – Drift between top and bottom of the block

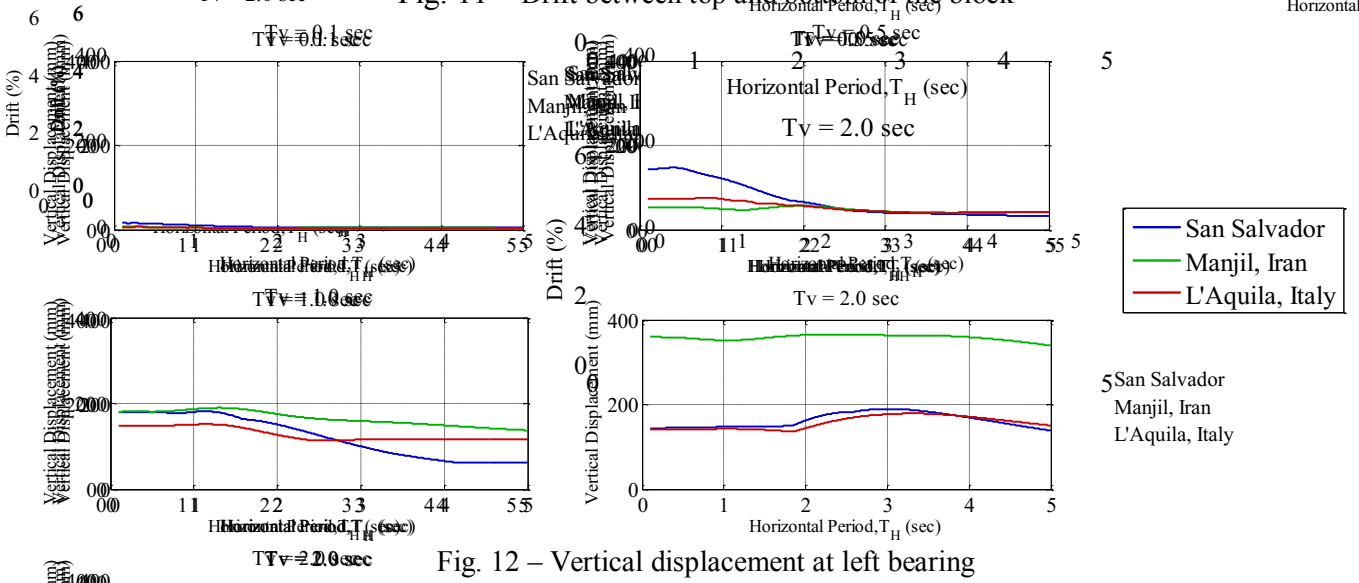

Fig. 12 – Vertical displacement at left bearing

Horizontal acceleration amplification factors (horizontal peak absolute acceleration normalized by horizontal peak ground acceleration or PGA) are illustrated in Fig. 13 and Fig. 14 for the top and base of the block, respectively. In addition, the vertical acceleration amplification factor (vertical peak absolute acceleration normalized by vertical PGA) at the left bearing is presented in Fig. 15. The acceleration at the top exceeds the base acceleration in case of stiff structure with $T_H \leq 1.0$ sec and $T_V = 0.1$ sec. Otherwise, the top acceleration is lower than the base acceleration. The horizontal acceleration attenuates as T_H increases; and the effect of shifting T_V on the horizontal acceleration is not significant after a certain limit of T_H (Fig. 13 and Fig. 14). In the range of typical horizontal isolation ($T_H \geq 2.0$ sec), the horizontal acceleration is independent of the vertical period. For example, at $T_H = 3.0$ sec, the horizontal acceleration at both top of the block and bearing is almost 0.25 times the horizontal PGA regardless of vertical period. In the range of typical horizontal isolation periods ($T_H \geq 2.0$ sec), the vertical acceleration is not affected by T_H variation, and is inversely proportional to T_V as observed in Fig. 15. Vertical acceleration attenuation can be achieved by increasing T_V to make the bearings more flexible for movement; therefore, the controlling parameter is the vertical displacement.

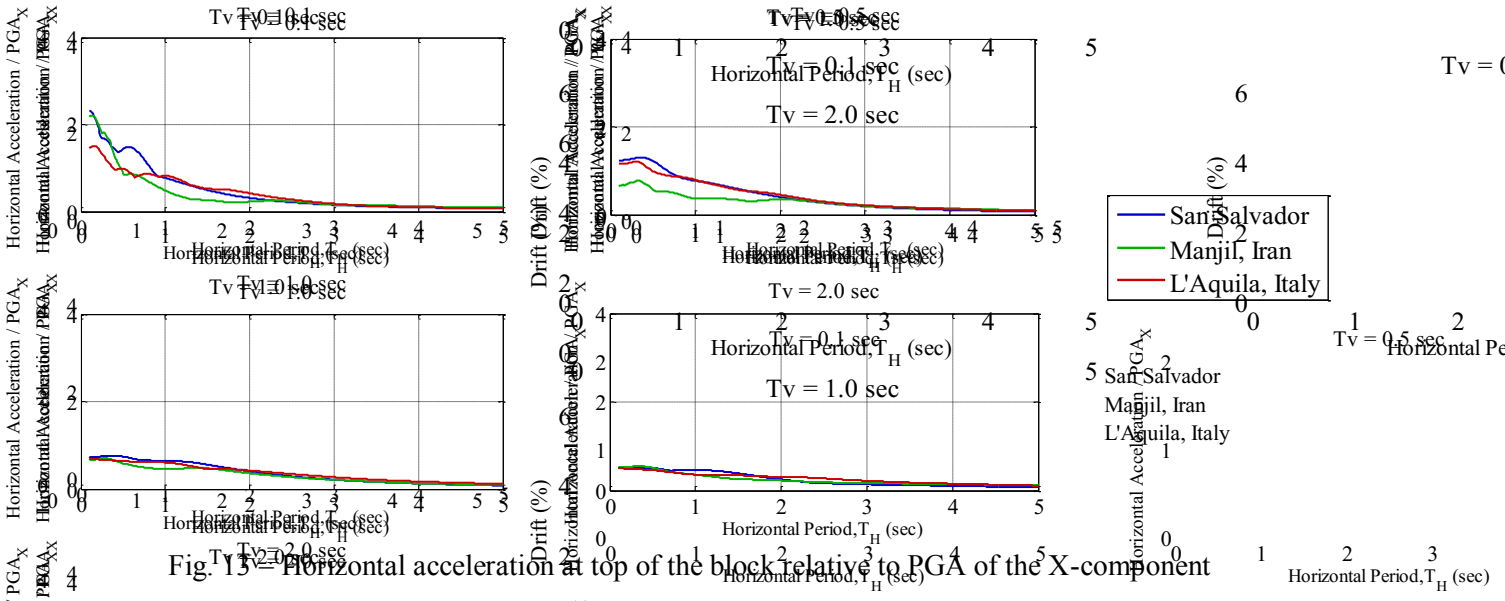

Fig. 13 – Horizontal acceleration at top of the block relative to PGA of the X-component

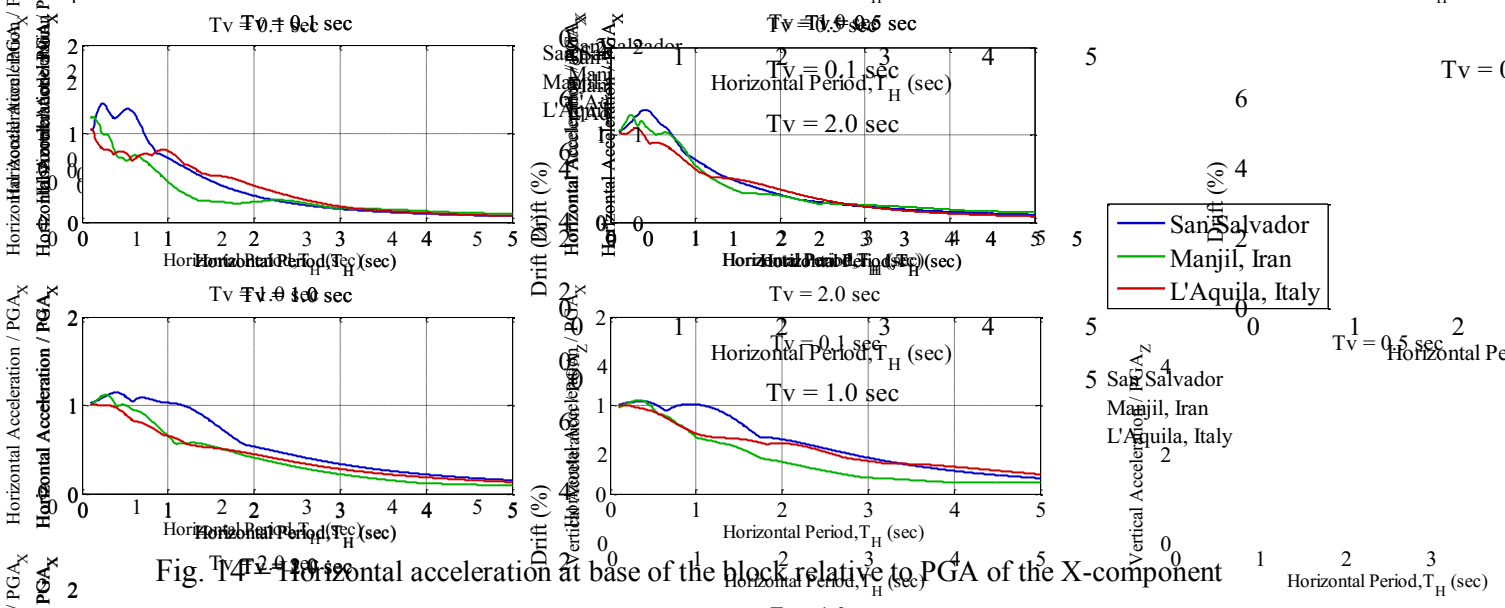

Fig. 14 – Horizontal acceleration at base of the block relative to PGA of the X-component

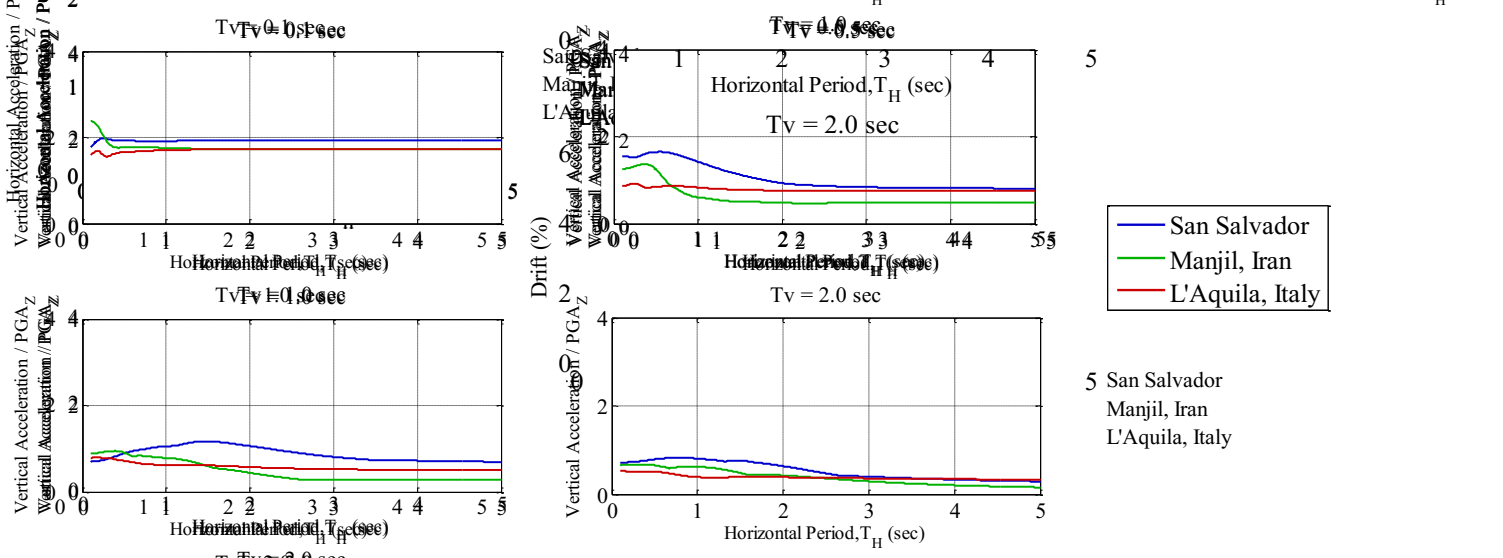

Fig. 15 – Vertical acceleration at left bearing relative to PGA of the Z-component

5. Conclusion

The simplified 2D rigid block model was used to explore the fundamental dynamic behavior of a 3D isolated structure subjected to horizontal and vertical ground motion excitation. The model results led to a number of useful observations.

1. The coupling between horizontal translation and the block rotation increases with increasing T_V, which leads to increasing rotation and consequently top horizontal displacement increases and bearing horizontal displacement decreases.
2. Large drifts result even at low T_H when vertical flexibility is introduced (T_V = 0.5, 1 or 2 sec). The drift ratio is maximized approximately when $T_H = T_V$. However, the drift ratio always decreases as T_H increases beyond T_V. This suggests that for effective design, T_H and T_V should not be closely coupled, and T_H should be selected to be much longer than T_V.
3. According to ASCE drift limits, T_V = 0.5 sec produces aceptable results for almost all T_H, T_V = 1.0 sec produces aceptable drifts for $T_H > 3$ to 4 sec, and T_V = 2 sec produces drift higher than ASCE limit for all values of T_H.
4. The vertical displacement U_Z takes the exact shape of the vertical mode coordinate $q_3(t)$ (q_2 when T_V = 2 sec), and increases in amplitude while decreasing in frequency as T_V increases.
5. Bearings vertical displacement increases with the increase of $_{TV}$; however, it is almost independent of T_H except for the short period range when T_V = 0.5 and 1.0 sec, during which vertical displacement at the bearings decreases as T_H increases.
6. In the range of typical horizontal isolation ($T_H \geq 2.0$ sec), the horizontal acceleration is independent of T_V and vertical acceleration is independent of T_H. Therefore, for both horizontal and vertical directions, acceleration attenuation can be achieved by increasing the isolation period to make the bearing more flexible for movement; however, the controlling parameter is the displacement.

Preliminary results suggest that vertical isolation periods as low as 0.5 seconds will be effective in attenuating the vertical acceleration. Limiting the vertical isolation period will make design of a 3D isolation system more feasible with respect to vertical displacement capacity and avoiding rocking.

6. Acknowledgements

This material is based upon work supported by the National Science Foundation under Grant No. CMMI 1437003. Any opinions, findings, conclusions or recommendations expressed in this publication are those of the authors and do not necessarily reflect the views of National Science Foundation.

7. References

[1] Ryan KL, Soroushian S, Maragakis E, Sato E, Sasaki T, Okazaki T (2016): Seismic simulation of an integrated ceiling-partition wall-piping system at E-Defense. I: Three-dimensional structural response and base isolation. *Journal of Structural Engineering*, **142** (2), 04015130-1-15.

[2] Furukawa S, Sato E, Shi Y, Becker T, and Nakashima M (2013): Full-scale shaking table test of a base-isolated medical facility subjected to vertical motions. *Earthquake Eng. Struct. Dyn*., **42**(13), 1931–1949.

[3] Inoue K, Fushimi M, Moro S, Morishita M, Kitamura S, Fujita T(2004): Development of three-dimensional seismic isolation system for next generation nuclear power plant. *13th World Conference on Earthquake*, Vancouver, B.C., Canada, Paper No. 3445.

[4] Suhara J, Tamura T, Ohta K, Okada Y, Moro S (2003): Research on 3-D base isolation system applied to new power reactor 3-D seismic isolation device with rolling seal type air spring: Part 1. *Transaction of the 17th International Conference on Structural Mechanics in Reactor Technology*, Prague, Czech Republic, Paper # K09-4.

[5] Suhara J, Matsumoto R, Oguri S, Okada Y, Inoue K, Takahashi (2005): Research on 3-D base isolation system applied to new power reactor 3-D seismic isolation device with rolling seal type air spring: Part 2. *18th International Conference on Structural Mechanics in Reactor Technology*, Beijing, China, Paper # K10-3.

[6] Kageyama M, Iba T, Umeki K, Somaki T, Moro S (2003): Development of three-dimensional base isolation system with cable reinforcing air spring. *Transaction of the 17th International Conference on Structural Mechanics in Reactor Technology*, Prague, Czech Republic, Paper #K09-5.

[7] Kageyama M, Iba T, Umeki K, Somaki T, Hino Y, Moro S, Ikutama S (2004): Study on three-dimensional seismic isolation system for next generation nuclear power plant: independent cable reinforced rolling-seal air spring. *13th World Conference on Earthquake Engineering*, Vancouver, B.C., Canada, Paper# 1346.

[8] Kashiwazaki A, Shimada T, Fujiwaka T, Moro S (2003): Study on 3-dimensional base isolation system applying to new type power plant reactor (hydraulic 3-dimensional base isolation system: No.1). *Transaction of the 17th International Conference on Structural Mechanics in Reactor Technology*, Prague, Czech Republic, Paper #K09-2.

[9] Suhara J, Matsumoto R, Torita H, Tsuyuki Y, Kamei T, Takahashi O, Kunimatsu Y, Aida H, Fujita T (2008): Construction of civil building using three dimensional seismic isolation system: Part 2, Tests for three dimensional seismic isolation system. *14th World Conference on Earthquake Engineering*, Beijing, China.

[10] Takahashi O, Aida H, Suhara J, Matsumoto R, Tsuyuki Y, Fujita T (2008): Construction of civil building using three dimensional seismic isolation system: Part 1, Design of building using three dimensional seismic isolation system. *14th World Conference on Earthquake Engineering*, Beijing, China

[11] Li X, Xue S, Cai Y (2013): Three-dimensional seismic isolation bearing and its application in long span hangars. *Earthquake Engineering and Engineering Vibration*, **12 (1)**, 55-65.

[12] Xu ZD, Huang XH, Lu LH (2012a): Experimental study on horizontal performance of multi-dimensional earthquake isolation and mitigation devices for long-span reticulated structures. *Journal of Vibration and Control*, **18** (7), 941-952.

[13] Xu ZD, Tu Q, Guo, Y F (2012b): Experimental study on vertical performance of multi-dimensional earthquake isolation and mitigation devices for long-span reticulated structures", *Journal of Vibration and Control*, **18** (13), 1971-1985.

[14] Zhou Z, Wong J, Mahin S (2016): Potentiality of Using Vertical and Three-dimensional Isolation Systems in Nuclear Structures. *Nuclear Engineering and Technology*, http://dx.doi.org/10.1016/j.net.2016.03.005

[15] American Society of Civil Engineers (ASCE) (2010): *ASCE Standard – ASCE/SEI 7-10: Minimum design loads for buildings and other structures*. Reston, VA.

[16] National Earthquake Hazards Reduction Program (NEHRP) (2009): *Recommended Seismic Provisions for New Buildings and Other Structures*. FEMA P-750 / 2009 Edition.